

1. Data Preparation

Dataset Analysis A total of 60 different data were given, which corresponded to 10 different trials on 6 different objects. The objects tested were acrylic, black foam, car sponge, flour sack, kitchen sponge, and steel vase. Each of the trials consisted of data for Electrode Impedance, High Frequency Fluid Vibrations(pac), Low Frequency Fluid Pressure(pdc), Core Temperature Change (tac), Core Temperature (tdc), Robot arm joint effort (JEff), and Robot arm joint velocity (JVel).

Time Instance Selection The goal here was to select the perfect time to differentiate the objects using the pressure, vibration, temperature, and electrode data. After plotting the values for different objects and different trials, the time 500 was selected. This was because the time near 500 700 had the most stable and consistent data for all samples. For example, the pressure values had a lot of fluctuations around time 0 300 and 900 1000, implying that the pressure value in this range would be unhelpful in uniquely identifying the object. A sample of this is shown in Figure 1, with all trials for 4 different objects shown for the pressure value. Afterwards, the 19 electrode values were also used to select the time instance. Similarly, the time instance fluctuated between 0 50 and remained stable around afterwards. This resulted in the time instance 600 being selected, as 550 650 were all similar values for all instances, making this value robust to slight shifts in time.

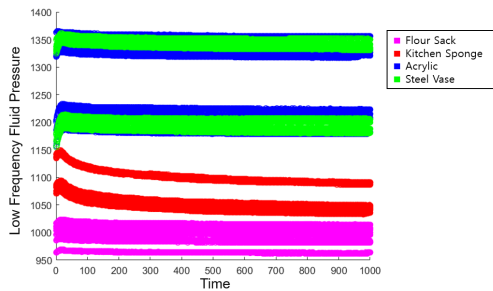


Figure 1. Pressure for All 10 Trials for Different Objects

PVT Analysis at Time 600 The PVT were plotted for different objects at time 600. This is shown in Figure 2. The same color to object mapping is to be used for all plots onwards.

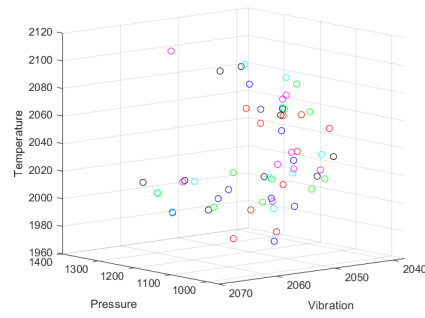


Figure 2. PVT Plot for 6 Different Objects for All Trials at Time 600

2. Principal Component Analysis (PCA)

PCA on PVT Data To use PCA, we must begin by standardising the data. Then we find the covariance

matrix:
$$\begin{bmatrix} Cov(P, P) & Cov(P, V) & Cov(P, T) \\ Cov(P, V) & Cov(V, V) & Cov(T, V) \\ Cov(P, T) & Cov(T, V) & Cov(T, T) \end{bmatrix} =$$

$$\begin{bmatrix} 1 & -0.2001 & -0.4578 \\ -0.2001 & 1 & 0.2630 \\ -0.4578 & 0.2630 & 1 \end{bmatrix}.$$
 Using the covariance matrix, we find the eigenvalues and

eigenvectors:
$$\begin{bmatrix} 0.5365 & 0 & 0 \\ 0 & 0.8347 & 0 \\ 0 & 0 & 1.6288 \end{bmatrix}$$
 and

$$\begin{bmatrix} -0.6687 & 0.4204 & -0.6132 \\ 0.1271 & 0.8773 & 0.4629 \\ -0.7326 & -0.2316 & 0.6401 \end{bmatrix}.$$
 Leaving the first column as it has the lowest eigenvalue, we attain the feature

vector:
$$\begin{bmatrix} 0.4204 & -0.6132 \\ 0.8773 & 0.4629 \\ -0.2316 & 0.6401 \end{bmatrix}.$$
 By projecting the selected

feature vectors onto the data (i.e. PVT Data x Feature vector), we obtained a 2D representation of the data. This is shown in Figure 3.

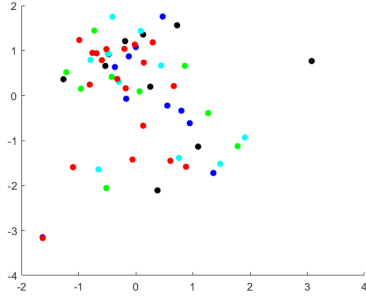


Figure 3. Re-plotting as 2D graph on selected PCs

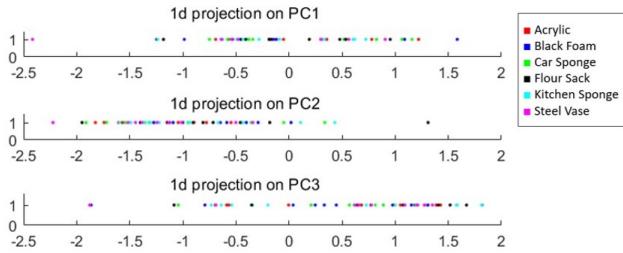


Figure 4. 1D Projection onto each Principle Component

Furthermore, we could see how each principle component distributes the data points as shown in Figure 4. This figure illustrates the data distribution, with each plot representing a principle component.

Comment on PVT Results Unfortunately, we don't see much of a trend in the 2D representation on Figure 3. However, we do see a cluster around (0.5,1) and another cluster around (1,-1). Furthermore, looking at the 1D representation of the data, we can see why the two clusters are shown in the 2D data. Looking at the graph for PC1, we see two different clusters, one around -0.3 and another around 0.8. On the other hand, PC2 has one cluster focused around -1. This can be seen in the x-axis and y-axis of the 2D graph, with the intersection of these two represented as the cluster in the 2d graph.

PCA on Electrode Data A similar process was followed to reduce the dimensionality of the Electrode Data. However, as the electrode data was 6x10x19 dimensions (6 objects, 10 trials, 19 data points), it was much more difficult to visualise. Figure 5 illustrates the principle components in decreasing variance order, and the first 3 principle components were selected to represent the data in 3D. Similar to the previous process of finding the new representation, the product of the electrode data and the feature vector (19x3 matrix) made of the top 3 principle components was used.

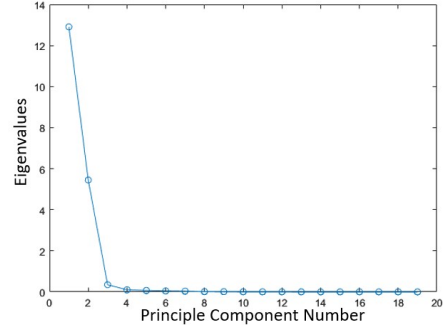


Figure 5. Electrode Data Scree Plot of All Principle Components

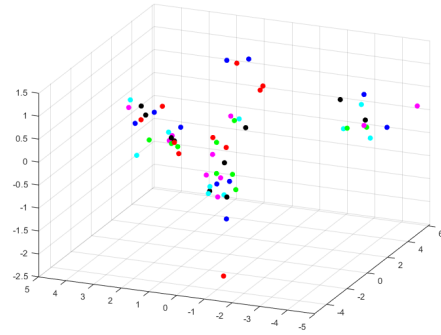


Figure 6. Electrode Data using 3 Principal Components with Largest Variance

The result is illustrated in Figure 6. The representation in 3D shows that the data were grouped into multiple clusters; however, it seemed to lack a correlation with the object type.

Comment on Electrode Results The representation in 3D shows that the data were grouped into multiple clusters. The scree plot illustrates the distribution of variance across the different principle components. As expected, the variance decreases in an exponential decay. Considering the scree plot, it is evident that choosing a 3D representation was the right choice. This is because all the principle components after the 3rd component decays into a practically 0 value. This is expected, as there are only 10 trials per object, leaving us with only a total of 60 data points, which is definitely too small for any higher dimensional representations. Furthermore, the 3D representation does illustrate some clustering, suggesting that the components have successfully reduced dimensions.

3. Linear Discriminant Analysis (LDA)

Black foam VS Car sponge, LDA for 2 axes Upon two objects, Black Foam and Car Sponge, LDA has been performed for 2 parameters each time, Pressure vs Vibration.

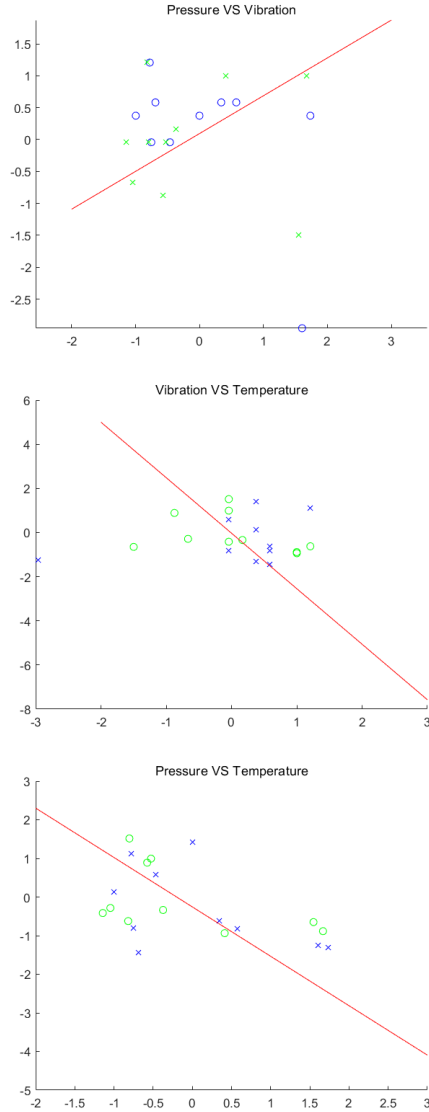


Figure 7. 2D LDA for PV, VT, PT

tion, Vibration vs Temperature, and Pressure vs Temperature. Firstly, the mean of each class (black foam and car sponge) has been calculated, as well as the total mean of both classes. From there, Scatter matrix within each class (S_w) and Scatter matrix between the classes (S_b) have been calculated. Eigenvectors with their respective eigenvalues have been calculated with the $\text{eig}(\text{inv}(S_w) * S_b)$ function. The non-zero and highest eigenvalues have been selected for feature vector. These eigenvectors form LDA axes for projection.

3D LDA on PVT In 3D Linear Discrimination Analysis, 2 eigenvectors found were associated with eigenvalue of 0, meaning that some of the parameters were not useful in dis-

criminating between black foam and car sponge. This could be the case because they have similar textures, therefore the pressure of touch could have been similar and have limitations in discriminating between the two classes. The feature vector only includes one eigenvector with a non-zero eigenvalue, therefore showing a linear line separating the classes in the 3D space.

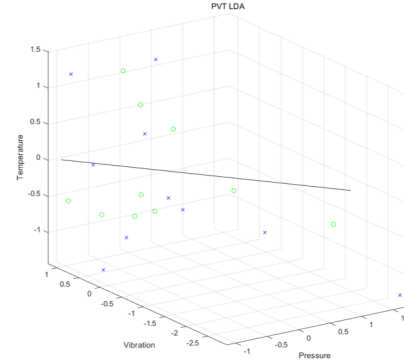


Figure 8. 3D LDA between Black Foam and Car Sponge

LDA with Steel Vase and Flour Sack Referring to Figure 1, the flour sack and steel vase has a clear distinction between its pressures. Also assuming from the nature of its material, the temperature and vibration measurements are likely to vary. Steel vase would be colder, while flour sack will have higher temperature measurements. For clear distinction via LDA, I have chosen steel vase and flour sack as the two objects for LDA.

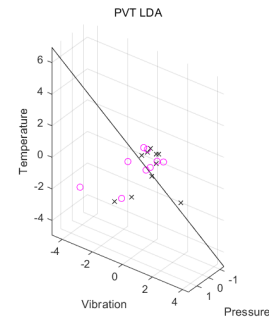


Figure 9. 3D LDA between Flour Sack and Steel Vase

However it was shown that it resulted in 2 eigenvectors related to eigenvalue of 0. The difference in the parameters is still relatively weak, resulting in poor discrimination with only 1 LDA axis in the 3D space.

4. Clustering & Classification

4.1. Clustering

K-means Clustering K-means clustering was adopted, with $k=6$ (6 clusters). This is because we were provided with 6 different objects.

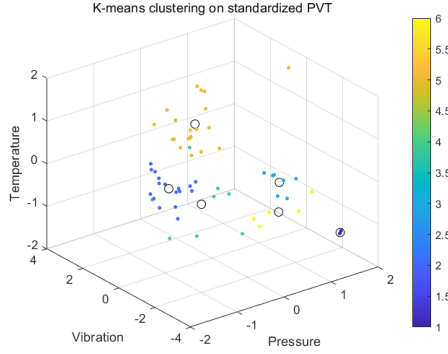


Figure 10. K-means clustering on standardized PVT

As shown in Figure 10, the clusters are reasonable, with data points close to each cluster mean being classified as the same cluster correctly. However, it shows some dissimilarity with the real-life object clusters or actual distribution of different objects in the 3D PVT space, as shown in Figure 2.

Different distance metrics on K-means clustering

Square euclidean, Manhattan, cosine distance metrics have been tested. With different distance metrics, the method of measuring from the cluster means to the data points changes. Since K-means clustering is a method to update the data point to the closest cluster mean, with different metrics, the cluster mean or the cluster centers change. Therefore, the cluster distributions change as well. The K-means clustering using Manhattan distance metric is shown in the Figure 11.

4.2. Bagging

Decision Trees The number of decision trees used was 100000. This was to improve the accuracy of the bagging by using more trees to make the decision. Figure 12 in the Appendix shows the visualization of two decision trees used in the bagging.

Bagging on Electrode Data The result is shown in Figure 13 in Appendix, with an accuracy of 16.7%. The PCA has definitely been helpful in terms of dimensionality reduction for faster and simpler bagging process. However, it is hard to say that it helped the accuracy, as the PCA wasn't too successful in accurately representing and grouping the

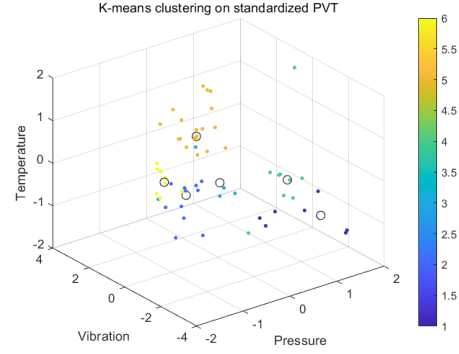


Figure 11. K-means clustering on Manhattan distance metric

different objects either. Given that certain objects may have similar senses; for instance, car sponge and kitchen sponge being almost identical, this would be difficult to classify. An attempt at the same method using time instance 1 is mentioned in the conclusion, with better results.

5. Conclusion

PCA was useful in the dimension reduction of large-dimensional data such as the electrode measurement data, which had 19 dimensions. Also, LDA allowed for projection onto new axes for classification. However, during LDA, most eigenvectors were identified with close-to-zero eigenvalues. This could be due to some materials not showing a significant difference in PVT. The reasons could be the objects sharing similar textures, or real-life errors that occurred during the collection of the data.

Overall, it was difficult to classify which object was being grasped only using touch. The analysis may be improved by using more samples or implementing data cleaning such as outlier removal. Selecting another time instance for PVT analysis could also produce a better result, as a repetition in the experiment using electrode data proved to give better results in the case of an earlier time instance between 0 10. The confusion matrix from using time instance 1 is given in the appendix in 14. Still, the accuracy wasn't good enough to conclude that the electrode data is enough to detect what object is being grasped.

For a cheap tactile sensor, it could be more important to measure the pressure data. From section A, different materials with distinctive textures showed very different pressure values, allowing for differentiation. Meanwhile, classification using electrode values was difficult.

Another method to approach this would be using more than one time instance, potentially as different features. An advantage for this would be that fewer sensors are required implying a cheaper price. Also, using multiple time instances may bring better results as there are much more data points.

6. Appendix

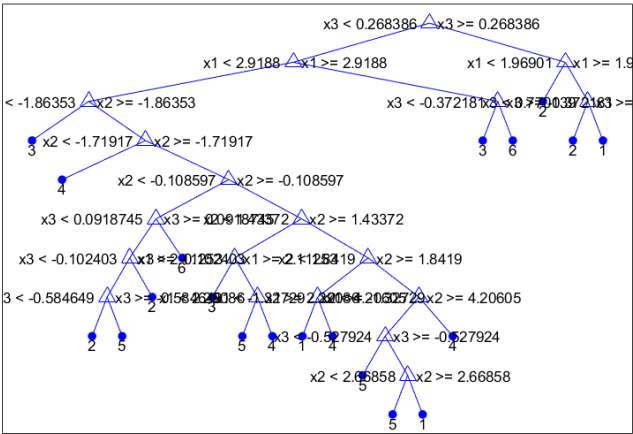
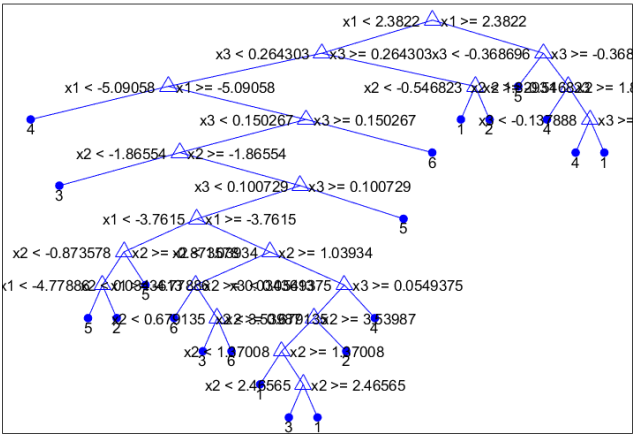


Figure 12. Visualization of Two Decision Trees

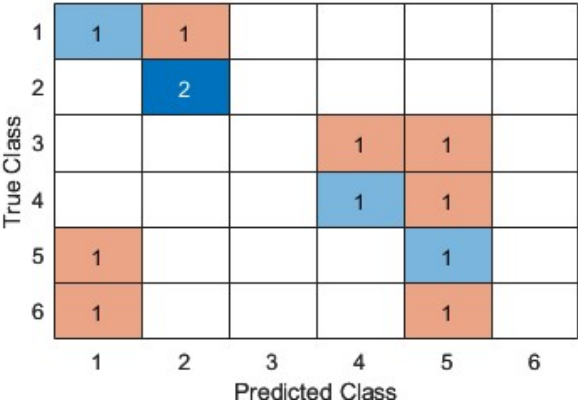


Figure 14. Confusion Matrix From Bagging Using Time Instance of 1

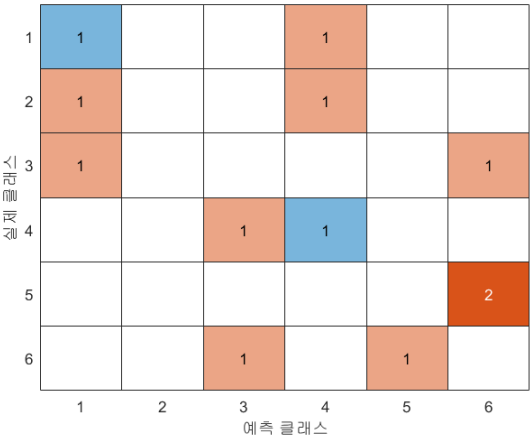


Figure 13. Confusion Matrix Results